Solar Energy Materials & Solar Cells 92 (2008) 1366–1372

Contents lists available at ScienceDirect

Solar Energy Materials & Solar Cells

journal homepage: www.elsevier.com/locate/solmat

Properties of fluorine doped ZnO thin films deposited by magnetron sputtering

H.S. Yoon [a], K.S. Lee [a], T.S. Lee [a], B. Cheong [a], D.K. Choi [b], D.H. Kim [c], W.M. Kim [a,*]

[a] Thin Film Materials Research Center, Korea Institute of Science and Technology, 39-1, Hawolgok-dong, Sungbuk-gu, Seoul 136-791, Republic of Korea
[b] Department of Ceramic Engineering, Hanyang University, 17 Haengdang-dong, Sengdong-gu, Seoul 133-791, Republic of Korea
[c] Division of Materials Science and Engineering, Korea University, 5-1 Anam-Dong, Sungbuk-gu, Seoul 136-701, Republic of Korea

ARTICLE INFO

Article history:
Received 6 March 2007
Received in revised form
14 April 2008
Accepted 19 May 2008
Available online 26 June 2008

Keywords:
Fluorine doped ZnO film
Transparent conducting oxide
Magnetron sputtering
Vacuum-annealing

ABSTRACT

Fluorine doped ZnO (FZO) films were deposited on Corning glass by radio frequency (rf) magnetron sputtering of pure ZnO target in CF_4 containing gas mixtures, and the compositional, electrical, optical, and structural properties of the as-grown films as well as the vacuum-annealed films were investigated. The fluorine content in FZO films increased with increasing CF_4 content in sputter gas. FZO films deposited at elevated temperature of 150 °C had considerably lower fluorine content and showed a poorer electrical properties than the films deposited at room temperature. Despite high fluorine contents in the films, for all the FZO films, the carrier concentration remained below $2 \times 10^{20}\,cm^{-3}$, leading to fairly low doping efficiency level. Vacuum-annealing of the FZO films deposited at room temperature resulted in substantial increase of Hall mobilities, reaching as high as $43\,cm^2/Vs$. This was attributed partly to the removing of oxygen vacancies and/or the forming chemical bonds with interstitial zinc atoms by fluorine interstitials and partly to the passivation effect of excess fluorine atoms by filling in the dangling bonds at the grain boundaries. For all the films with thickness of around 300 nm, the optical transmissions in visible were higher than 80%, and increased with increasing fluorine content up to 85% for the film with highest fluorine content.

1. Introduction

Due to recent soar in low material cost of indium, the need for substitution of tin doped indium oxide (ITO) which became major drain of indium consumption is ever increasing [1]. Among many transparent conducting oxide (TCO) materials, doped ZnO has been attracting a great deal of attention as an alternative for ITO due to its low material cost and non-toxicity not to mention its low electrical resistivity and good optical transparency in the visible region [2,3]. Much more interest has been given to TCOs based on ZnO such as undoped ZnO [4] and Al doped ZnO (AZO) [5,6] due to their stability under hydrogen plasma which makes them a potent candidate for solar cell technology based on thin film silicon. Also, Ga doped ZnO (GZO) films has received recent attention due to their low electrical resistivity [7,8]. Unlike the abundant studies on ZnO films doped with cation dopants such as Al, Ga, or B, only a few investigations, in which fluorine was used as anion dopant, can be found in literature. Instead of doping cations, Fu et al. obtained a noteworthy result by doping fluorine to ZnO (FZO) films by using a chemical vapor deposition (CVD) technique [9]. The electrical resistivity of $6 \times 10^{-4}\,\Omega cm$ and Hall mobility as high as $40\,cm^2/Vs$ were reported for the CVD-grown FZO films. The low resistivity of the FZO films is mostly due to their high mobility, and was attributed to the substituted fluorine into oxygen sites which mainly perturbs the valence band, thereby leaving the conduction band relatively free of scattering [10]. Gordon et al. reported a test result in which the FZO films grown by CVD gave better cell performance than fluorine doped SnO_2 (FTO) films when applied for transparent electrodes in thin film silicon solar cell [11]. Despite the beneficial effect of fluorine doping, there have not been much subsequent reports regarding fluorine doped ZnO films. Olvera et al. studied the doping of fluorine into ZnO by spray pyrolysis technique, but the electrical properties were far from satisfactory [12,13]. On the other hand, Miyata et al. [14] and Minami et al. [15] reported possibility of fabricating fluorine doped ZnO and fluorine and gallium co-doped ZnO films with better electrical properties by using vacuum arc plasma evaporation (VAPE), but no detailed analysis has been given. Recently, Xu et al. reported that FZO films with low electrical resistivity of $7.95 \times 10^{-4}\,\Omega cm$ and a good optical transparency could be fabricated by performing an appropriately controlled annealing of ZnF_2 films, which were deposited by electron-beam evaporation, in oxygen atmosphere [16]. High Hall mobility value of $46\,cm^2/Vs$ was tagged.

* Corresponding author. Tel.: +82 2 958 5384; fax: +82 2 958 5509.
E-mail address: wmkim@kist.re.kr (W.M. Kim).

0927-0248/$ - see front matter © 2008 Elsevier B.V. All rights reserved.
doi:10.1016/j.solmat.2008.05.010

Despite wide usage of magnetron sputtering technique in fabrication of TCO films, no study has been reported on the fluorine doped ZnO films deposited by sputtering technique. In this study, FZO films were formed by using planar magnetron sputtering of pure ZnO target in gas mixtures containing CF_4, their compositional, electrical, optical, and structural properties were examined. Also, the effect of vacuum annealing on the FZO films together with the results observed by a real-time monitoring of resistance changes during the heating and cooling period in vacuum were discussed.

2. Experimental details

FZO films with varying fluorine content were deposited on glass substrates (Corning Eagle 2000) by radio frequency (rf, 13.56 MHz) planar magnetron sputtering of 2-in ZnO target. The fluorine doping was done by introducing a mixed gas of pure Ar and CF_4 into the sputtering chamber while sputtering pure ZnO target. FZO films with three different fluorine contents were prepared and their properties were compared with those of undoped ZnO film. Three FZO films prepared by using different volumetric flow rates of CF_4 gas of 0.1, 0.4, and 0.8 vol% will be referred to as FZO1, FZO4, and FZO8, respectively, in an order of increasing CF_4 content in sputtering gas mixtures. Film thickness was kept at around 300 nm for all the films by controlling the deposition time according to the predetermined deposition rates which were measured from the films deposited on strip-masked substrates using a profilometer (KLA-tencor, ASIQ). The base pressure in the chamber was below 5×10^{-5} Pa, and the sputtering deposition was carried out at a pressure of 0.13 Pa. The rf power on target was kept at 50 W, and the distance between the target and the substrate was 50 mm. The substrate was not intentionally heated unless specified otherwise, and rotated at a constant speed of 12 rpm during sputtering. Annealing experiment was performed in a specially designed apparatus which can be pumped down to below 10^{-4} Pa and are equipped with multiple probes for the real-time measurement of the resistance change during the heating and cooling cycles. Annealing treatments of the as-prepared films were carried out in vacuum of 10^{-4} Pa for 1 h. The maximum temperature attained was 310 °C, and heating rate was in 10 °C/min. And natural cooling without forcing was applied in vacuum.

For compositional analysis, Auger electron spectroscopy (AES) analysis was carried out. In order to make quantitative analysis, composition analysis by using Rutherford backscattering spectrometry (RBS) was performed on FZO8 sample which was expected to have the highest fluorine content among all samples, and the very same sample was then analyzed by using AES. By comparing both results, the sensitivity factor of each element was determined, and used for other AES analysis. The electrical resistivities, Hall mobilities, and carrier concentrations were determined from Hall-effect measurement equipment using a Van der Pauw method. Crystalline structures of the films were analyzed using an X-ray diffractometer (Rikaku, ATX-XRD, Cu K_α ($\lambda = 0.154056$ nm)) in thin film mode (incidence angle 1.5°). The optical transmission and reflection spectra were obtained on a UV–visible spectrophotometer (Perkin–Ellmer, Lambda 35) in wavelength ranges of 250–1100 nm.

3. Results

3.1. Compositional properties

Fig. 1 shows the variations of fluorine content in FZO films obtained by AES analysis. The fluorine contents in the as-grown FZO films increased with increasing CF_4 volume contents in sputtering gas, but in a little scattered manner. Vacuum annealing resulted in the reduction of fluorine content, the extent of decrease in fluorine content being larger for the films with larger fluorine contents in the as-deposited states. In one set of experiments, FZO films were deposited at elevated temperature of 150 °C in the same gas mixtures, and their compositional variations are also presented in Fig. 1. The fluorine contents in these films were significantly lower than those prepared at room temperature for a given gas composition. The fluorine content of FZO film deposited at 150 °C in gas mixture of 0.8 vol% CF_4 yielded only 1.72 at%, while that deposited at room temperature in the same gas mixture being as high as 7.36 at%. This temperature dependence of fluorine incorporation into ZnO films is somewhat different from those observed in In_2O_3 films [17]. Fluorine content in In_2O_3 films deposited by both placing InF_3 pallets on In_2O_3 target and introducing CF_4 gas mixtures decreased with increasing substrate temperature, but the temperature effect was not so pronounced as was observed in this study for ZnO films. Also, it has to be mentioned that the carbon contents in the FZO films deposited in CF_4 containing gas mixtures remained in noise level. Carbons introduced in the sputtering are thought to be pumped out by forming gaseous C–O bonds with very high dissociation energy of 1076 kJ/mol such as CO, CO_2, and COF_2 [18,19], to which oxygen species needed are provided from dissociation of ZnO. Deposition rate was the highest for the undoped ZnO film deposited in pure Ar, and decreased with increasing CF_4 content in sputter gas. The deposition rates of undoped ZnO, FZO1, FZO2, and FZO3 films were 8.3, 8.1, 7.4, and 6.7 nm/min, respectively. The deposition rate of FZO8 film lowered down to 80% of the undoped ZnO film. This significant reduction in deposition rate is attributed largely to the abovementioned etching-away reactions and, to a lesser extent, to the lowering of sputter yields caused by the addition of CF_4 gas.

3.2. Electrical properties

Fig. 2 summarizes (a) the electrical resistivities, (b) the carrier concentrations, and (c) the Hall mobilities of the undoped ZnO and FZO thin films plotted against the fluorine content in the film. The resistivity of the as-grown FZO films deposited at room

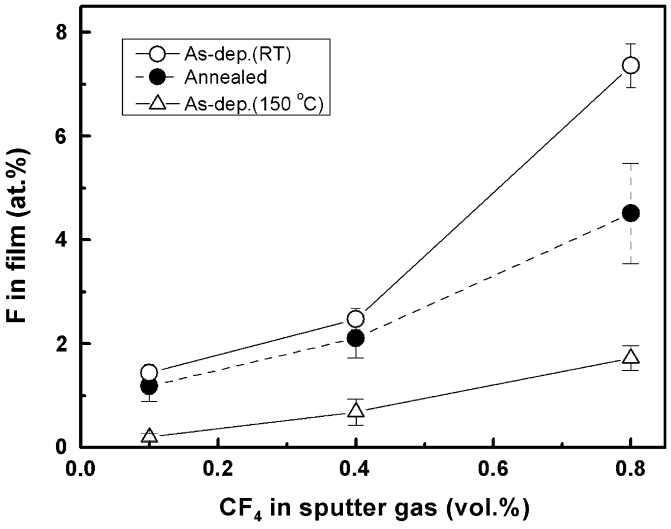

Fig. 1. Fluorine contents in FZO films with respect to CF_4 volume content in sputter gas. Open circles with solid line, closed circles with dashed line, and open triangles with solid lines represent the as-deposited films at room temperature, the vacuum-annealed films deposited at room temperature, and as-deposited at 150 °C, respectively.

temperature showed a typical valley-like behavior with respect to fluorine content in film, i.e. having minimum resistivity at intermediate fluorine content. For all the as-grown films, the carrier concentrations were relatively low and did not exceed $1.53 \times 10^{20}\,cm^{-3}$. The Hall mobilities of the undoped ZnO and FZO films deposited at room temperature were in the ranges 17–22 cm^2/Vs except for the FZO8 film with highest fluorine content. Vacuum-annealing of FZO films resulted in large drop of resistivity due to the increases of both the free carriers and the Hall mobility. Although the carrier concentrations increased due to annealing in vacuum, the absolute numbers were still remained at relatively low level, the highest carrier concentration being still less than $\sim 3 \times 10^{20}\,cm^{-3}$. Upon vacuum-annealing, however, substantially large increase in Hall mobility was observed for FZO films, reaching as high as 39 and 43 cm^2/Vs for FZO1 and FZO4 film, respectively. It is also notable that, for the undoped ZnO film, the electrical property was rather deteriorated after vacuum-annealing due to a large drop of carrier concentration combined with a slight decrease in Hall mobility.

The overall behavior of electrical properties observed in FZO films deposited at 150 °C with respect to fluorine contents is similar to that of the as-grown FZO films formed at room temperature. But the composition range is much narrower than the FZO films prepared at room temperature due to lower fluorine contents in these films as stated above. The electrical properties of FZO films fabricated at 150 °C were poorer than those grown at room temperature. The lowest resistivity of FZO films deposited at 150 °C was $4.4 \times 10^{-3}\,\Omega cm$ which is higher than 2.7×10^{-3} and $1.5 \times 10^{-3}\,\Omega cm$ observed for the as-grown FZO1 and the vacuum-annealed FZO4, respectively. Although the Hall mobility values of 30 and 21 cm^2/Vs were tagged for films deposited in gas mixtures with 0.1 and 0.4 CF_4 vol%, the corresponding carrier concentrations were only 3.3×10^{19} and $6.2 \times 10^{19}\,cm^{-3}$, respectively. One of the FZO film deposited at 150 °C in CF_4 content 0.8 vol%, which had the highest fluorine content among the films deposited at 150 °C, was annealed in vacuum and the resulting electrical property was examined. The as-deposited film had resistivity of $7.84 \times 10^{-2}\,\Omega cm$, Hall mobility of 4.7 cm^2/Vs, and carrier concentration of $1.7 \times 10^{19}\,cm^{-3}$. The resulting resistivity, Hall mobility and carrier concentration after vacuum-annealing were $3.6 \times 10^{-3}\,\Omega cm$, 30.5 cm^2/Vs and $5.6 \times 10^{19}\,cm^{-3}$, respectively. Although the degree of improvement was less than those observed in FZO films deposited at room temperature, the vacuum-annealing also resulted in an improvement of the electrical properties.

In Fig. 3, the results obtained from the real-time measurement of resistance change during the heating and cooling cycle for the undoped ZnO and FZO films deposited at room temperature. Initially, all the films showed a decreasing behavior of resistance with increasing temperature of up to about 250 °C, the absolute amounts of resistance change being different from film to film. But further increase in temperature resulted in clearly different behaviors depending on the fluorine content in films. A rather steep increase in resistance was observed for the undoped ZnO film. On the other hand, FZO8 films with highest fluorine content showed a totally reversed behavior, i.e. a rapid fall of resistance in temperature range 230–260 °C followed by slow decrease at higher temperature. FZO4 film exhibited a similar behavior to FZO8 film, the differences being the level-off of resistance at higher temperature and the absolute amount of resistance drop. The resistance of FZO1 film behaved intermediately, showing a slight rise of resistance at higher temperature. It is also worth mentioning that the resistance of the undoped ZnO film kept on increasing slowly even during the cooling period, while those of FZO films maintaining slowly decreasing tendency.

3.3. Optical properties

Comparison of the optical transmission and reflection spectra measured for the undoped ZnO and FZO8 films before and after vacuum-annealing is presented in Fig. 4. Absorption edge of the as-grown FZO8 film was located at higher energy side than that of undoped ZnO film. Also the overall transmission was higher for FZO8 film. For FZO8 film, vacuum-annealing resulted in blue shift of absorption edge, which reflects the increased free carrier concentration. In contrast, a very small red shift was observed for the undoped ZnO film. As is expected, the optical transmission

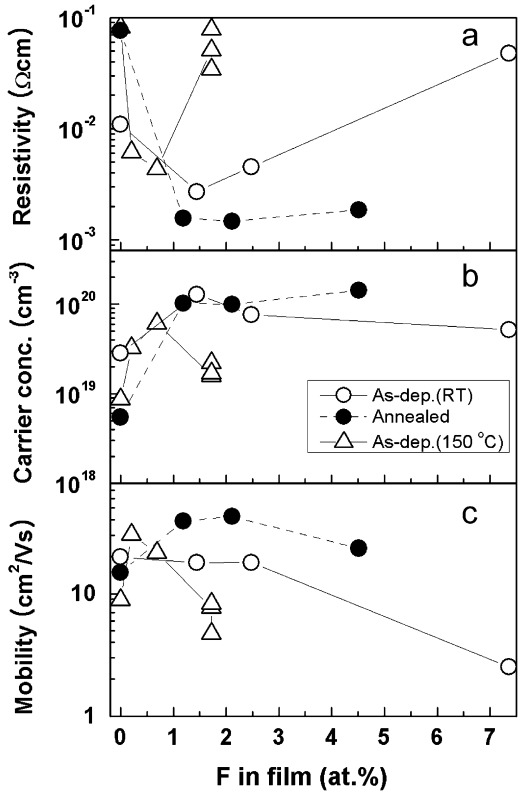

Fig. 2. Electrical properties of the as-deposited and the vacuum-annealed FZO films, (a) resistivities, (b) carrier concentrations, and (c) Hall mobilities. The symbol notations are the same as in Fig. 1.

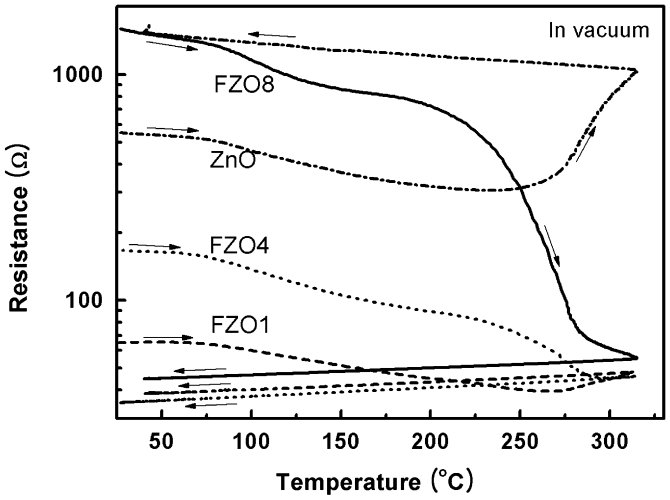

Fig. 3. Resistance changes of the undoped ZnO and FZO films deposited at room temperature during the heating and cooling cycle in vacuum.

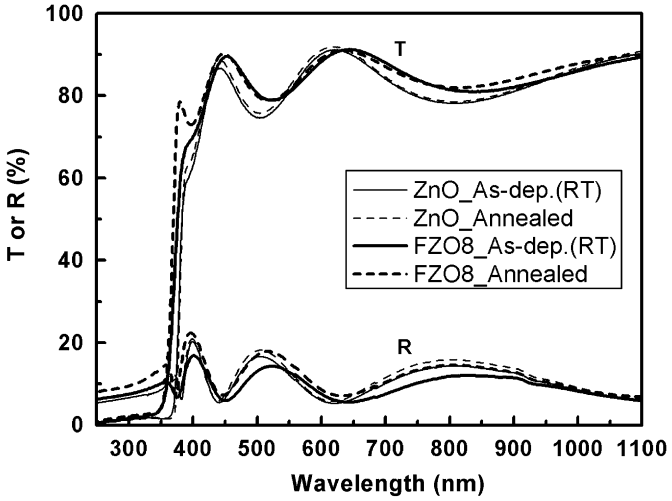

Fig. 4. Optical transmission and reflection spectra of the undoped ZnO and FZO8 films deposited at room temperature before and after vacuum-annealing.

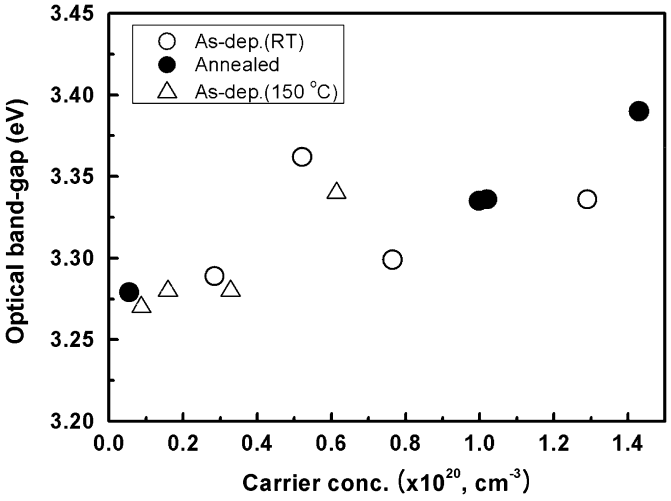

Fig. 5. Optical band-gap of the undoped ZnO and FZO films with respect to the carrier concentrations in the films. Open circles, closed circles, and open triangles represent the as-deposited films at room temperature, the vacuum-annealed films deposited at room temperature, and as-deposited at 150 °C, respectively.

and reflection spectra of FZO1 and FZO4 films showed an intermediate behavior, FZO1 being closer to the undoped ZnO and FZO4 being closer to FZO8. The transmittance values averaged in the spectral ranges 400–800 nm were 82.3%, 83.4%, 84.2%, and 84.9% in an increasing order of fluorine content in the as-grown films. The averaged transmittance of the undoped ZnO film increased about 1% upon vacuum-annealing, but those of FZO films did not show much increase. On the other hand, as shown in Fig. 4, a fairly large increase in reflection was observed for the vacuum-annealed FZO films, thereby reducing the overall absorption loss in the films. The average absorbance values of the vacuum-annealed ZnO, FZO1, FZO4, and FZO8 films were 5.7%, 5.4%, 3.9%, and 2.5%, respectively, indicating that absorption loss decreased with increasing fluorine content in the films.

Direct allowed band-gap of FZO films were evaluated optically by using relation of $\alpha h\nu \propto (h\nu - E_g)^{1/2}$ (for $h\nu > E_g$), where α is the absorption coefficient, h is Planck's constant, ν is frequency, E_g is band gap [20]. The absorption coefficient was evaluated from the spectroscopic optical data by adopting relationship which is defined with corrections for reflection loss at the front surface of the sample, i.e. $\alpha = (1/d)\ln[(1-R)/T]$, where d, T and R are the film thickness, transmission and reflection, respectively. The optical band-gaps of FZO films, which were estimated by plotting $(\alpha h\nu)^2$ versus. $h\nu$ and extrapolating the linear portion near the onset of absorption edge to the energy axis, are plotted in Fig. 5 as a function of carrier concentration. The optical band-gap exhibited an increasing tendency with increasing carrier concentration, showing a typical Burstein–Moss shift. For films with low carrier concentration, the magnitudes of optical band-gaps were lower than 3.3 eV which was reported for stoichiometric ZnO crystal [21]. This may be explained by the band-gap narrowing induced by self-energy shift originating from the displacement polarization and the interactions with the dopant atoms as explained by Sernelius et al. [22].

3.4. Structural properties

In Fig. 6(a), XRD profiles of the as-grown and the vacuum-annealed FZO films are plotted in 2θ ranges 29°–65°. Undoped ZnO film showed a strong peak from (0 0 2) plane located at 2θ position of about 34.4° together with a small peak from (1 0 3) plane at about 62.9°, indicating a typical hexagonal wurzite

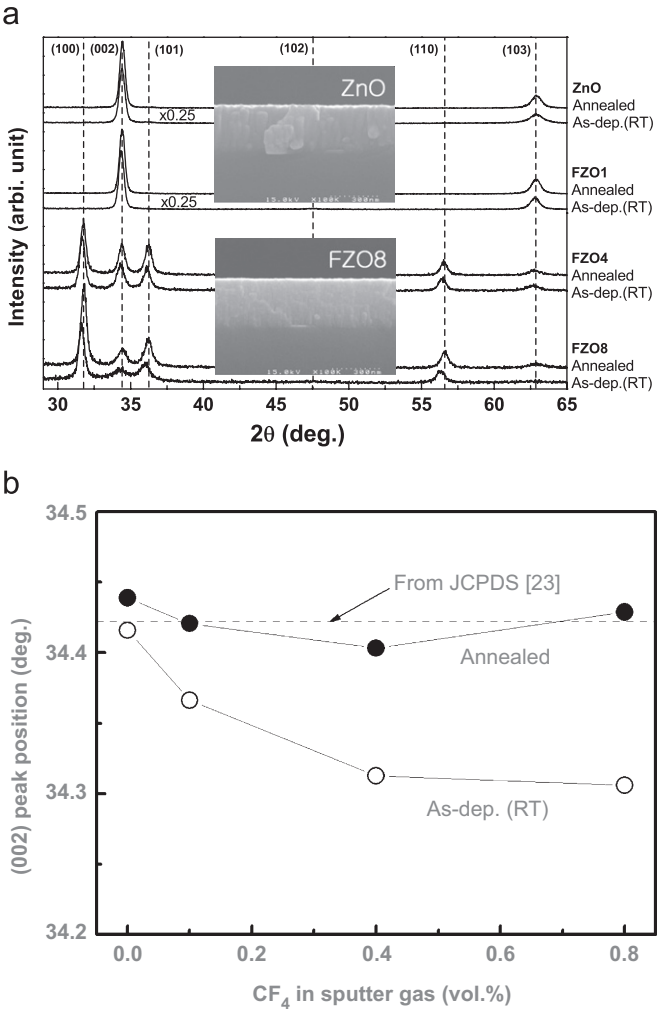

Fig. 6. (a) XRD profiles and (b) variations of (0 0 2) peak positions of the undoped ZnO and FZO films deposited at room temperature and vacuum-annealed. The relative peak intensities of the undoped ZnO and FZO films were reduced by a factor of 0.25. Upper and lower insets represent cross-sectional FE-SEM micrographs of the undoped ZnO and FZO8 films, respectively. Broken vertical lines drawn in (a) indicate 2θ position obtained from ZnO powder diffraction pattern [23], and broken horizontal line in (b) represents 2θ position of (0 0 2) peak.

structure with (0 0 2) preferred orientation. The dashed vertical lines drawn in the plot represent 2θ positions for ZnO powder diffraction patterns extracted from JCPDS table without specifying the relative intensity level [23]. The XRD profiles of the as-grown FZO1 film were almost the same as that of the undoped ZnO film, the only noticeable difference being slight shift of (0 0 2) peak position toward the lower angle side. With increasing fluorine content, the peak intensities from (0 0 2) and (1 0 3) planes diminished, instead the strong peaks from (1 0 0) and (1 0 1) planes together with weaker peak from (1 1 0) plane appeared, implying polycrystalline nature of FZO4 and FZO8 films. In Fig. 6(a), micrographs of cross-sectional view observed for the undoped ZnO and FZO8 films by using field-emission scanning electron microscopy are presented as insets. Course columnar structure is evident for the undoped ZnO film, and fine structure for FZO8 film. The grain size estimated by using well-known Sherrer relationship taking into account the instrumental broadening were 20, 21, 17, and 14 nm for undoped ZnO, FZO1, FZO4, and FZO8, respectively. Vacuum-annealing did not induce appreciable change in film structure, but fairly small but noticeable increases in peak intensities were observed, leading to slight increases in grain sizes of about 1–2 nm for all the films. Closer examination of Fig. 6(a) reveals, however, that peak positions of all the as-deposited FZO films are located at lower angle side of the corresponding reference peak positions indicated as the dashed vertical lines, and that the relative amounts of peak shift with respect to the reference peak positions increase with increasing fluorine content in the films (see Fig. 6(c) in which (0 0 2) peak positions before and after annealing are presented). Upon vacuum-annealing, all the peak positions moved towards the higher angle side, almost coinciding with the corresponding reference angle positions.

4. Disscusion

Although the vacuum-annealed FZO films deposited by magnetron sputtering gave significantly large Hall mobilities, the electrical resistivity values did not go down below $1\times10^{-3}\,\Omega$cm because of the low carrier concentrations. For the FZO films formed by CVD technique, Hu et al. reported the carrier concentration of about $5\times10^{20}\,cm^{-3}$ [9]. As long as the carrier concentration is concerned, the highest carrier concentration among the FZO films studied so far can be found from the work of Miyata et al. [14]. The carrier concentration of about $8\times10^{20}\,cm^{-3}$ with a moderate Hall mobility of about $10\,cm^2/Vs$ was observed for FZO film deposited at 100 °C by VAPE technique. The resulting resistivity was low, but this particular film did not have a good optical transparency [14].

Following the same definition of doping efficiency as used by Hu et al. [9], i.e. the ratio of the free carrier concentration to the atomic fluorine concentration, the calculated doping efficiency of FZO films are presented with respect to atomic fluorine content in Fig. 6. For comparison, the doping efficiency values, which were tabulated in the work of Hu et al. [9], are also presented in the plot. For the FZO films grown by CVD technique, even the lowest doping efficiency was 0.65, reaching as high as 0.97 for one film. On the other hand, the highest doping efficiency of FZO films obtained in this study was merely about 0.2, and the doping efficiency decreased with increasing fluorine content. In the calculation of doping efficiency, it was assumed that the free carriers were originated solely from the substituted fluorine atoms. Taking into account that ZnO film is known to possess usually such native donors as oxygen vacancies and zinc interstitials, practical doping efficiency would be substantially lower than the calculated ones. Also, it has to be mentioned that

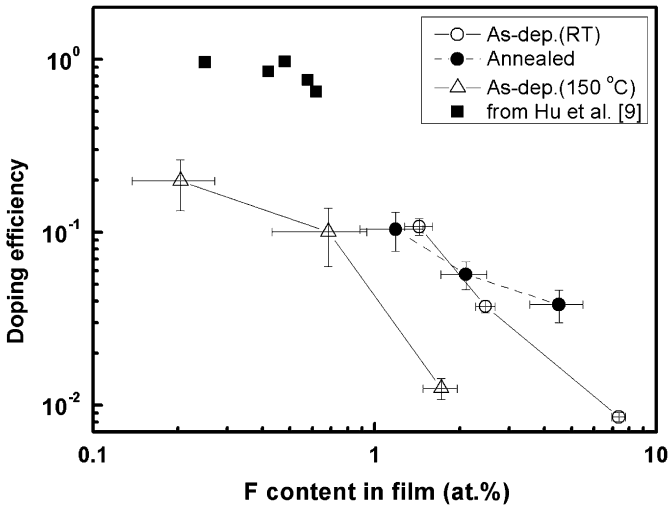

Fig. 7. Doping efficiencies of FZO films together with those of FZO films grown by CVD (closed rectangles) [9]. Open circles, closed circles, and open triangles represent the as-deposited films at room temperature, the vacuum-annealed films deposited at room temperature, and as-deposited at 150 °C, respectively.

the fluorine contents in FZO films grown by CVD were less than 1 at% which is much lower than most of fluorine contents in our films. Such low fluorine contents were also observed in FZO films deposited by spray pyrolysis technique [24]. The higher fluorine contents observed in our films are attributed to the non-equilibrium nature of sputter-deposition unlike the chemically activated processes. Although no detailed analysis on the fluorine content was made in the work of Miyata et al. [14], it is thought that their films would also contain somewhat large fluorine contents because their process is also typical physical vapor deposition and the source materials contained rather high ZnF_2 content (Fig. 7).

The low doping efficiency observed in FZO films in this study indicates that only small fraction of fluorine atoms substitute oxygen atoms, and that the excess fluorine atoms may be present in the form of interstitials, adsorbed (both chemically and physically) states at the grain boundaries, or secondary phase like ZnF_2. Considering that the XRD peak positions were shifted toward the lower angle side, that the relative amount of shift with respect to the reference peak position was increasing with increasing fluorine content, and that no peak from secondary phase such as ZnF_2 was observed in the XRD patterns, certain portion of the excess fluorine atoms are thought to be incorporated into films in the form of interstitials. Vacuum-annealing is considered to cause fluorine interstitials to fill oxygen vacancies and/or to form chemical bonds with interstitial zinc atoms, thereby removing interstitial defects. This effect of vacuum-annealing was evidenced by the observation made for the XRD peak positions for the annealed FZO films, in which peak positions shifted toward the corresponding reference peak positions of ZnO wurzite hexagonal crystallites. Substantial increase of the Hall mobilities upon annealing also supports the above deduction because the crystalline structure and the grain size in the annealed FZO films did not show much difference from those of the as-grown films. Some of the fluorine atoms adsorbed physically at the grain boundaries during deposition may be removed during the vacuum-annealing, resulting in reduction of fluorine content after annealing. The reduction in resistance observed for all the films during the initial heating in vacuum is related with stress relaxation and desorption of adsorbed oxygen at the grain boundaries. This was confirmed in an annealing experiment, in which the undoped ZnO and FZO8 films were

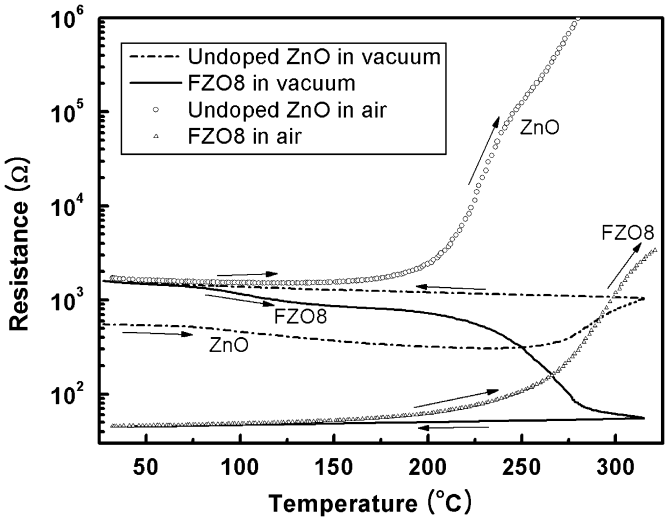

Fig. 8. Behavior of resistance change upon heating in air of the undoped ZnO and FZO8 films pre-annealed in vacuum.

heated up to 230 °C then cooled down in vacuum. For both films, the amount of reduced resistance during the heating period preserved during the cooling period, leading to the lowering of final resistance even for the undoped ZnO film. The rapid rise of resistance observed for the undoped ZnO film at higher temperature is thought to be due to removal of zinc interstitials [25,26].

It is also worth mentioning that the as-grown FZO films provide moderate Hall mobility values except for FZO8 film, and that all the annealed FZO films exhibit fairly high Hall mobility values despite the fact that the estimated grain sizes were in the ranges 14–22 nm. Xu et al. also reported very high Hall mobility of 46 cm^2/Vs in their study of FZO films with grain size of 21 nm, and ascribed it to a saturation mechanism of dangling bonds, which, otherwise, would drew O^{2-} and O^- resulting in increase of grain boundary potential barrier, at grain boundary by fluorine atoms [16]. Since the doping efficiency of the vacuum-annealed FZO films remained at low level, the excess fluorine atoms might exist as the adsorbed states by filling in the dangling bonds at the grain boundaries as presumed by Xu et al. [16]. In order to see the passivation effect of the adsorbed fluorine atoms at the grain boundaries, the undoped ZnO and FZO8 films, which were previously vacuum-annealed, were subsequently heated in atmosphere. The results in resistance changes are shown in Fig. 8 together with those of the previous vacuum-annealing shown in Fig. 4. Both films did not show decrease in resistance in initial period of heating. The resistance of the undoped ZnO film started to rise rapidly at temperature of about 200 °C. On the other hand, for FZO8 film, the resistance increased slowly, and the onset of rapid increase in resistance was delayed to temperature above 250 °C.

5. Conclusions

Fluorine doped FZO films were prepared on Corning glass by rf magnetron sputtering of pure ZnO target in gas mixtures containing CF_4 gas. Increase in CF_4 content in sputter gas resulted in increase of fluorine content in FZO films with carbon content remaining at noise level. Despite high fluorine content, all the as-grown FZO films exhibited relatively low level of the carrier concentrations. Undoped ZnO and FZO1 films with least fluorine content among the films showed a typical hexagonal wurzite structure with (0 0 2) preferred orientation, and FZO4 and FZO8 films with high fluorine content revealed polycrystalline fine structure. Fluorine incorporation into ZnO films deposited at high temperature was lower than that deposited at room temperature, and resulting film properties were poorer than those deposited at room temperature. Vacuum-annealing of FZO films deposited at room temperature resulted in improved electrical resistivities largely due to substantial enhancement of Hall mobility combined with slight increase in carrier concentration. No appreciable structural change was observed except for the relative shift of peak positions and very little increase in peak intensities. It was perceived that large portion of fluorine atoms incorporated into the as-deposited ZnO films exist in the form of interstitials and adsorbed states at the grain boundaries while a little amount being substituted for oxygen atoms, and that vacuum-annealing caused the fluorine interstitials to fill oxygen vacancies and/or to form chemical bonds with interstitial zinc atoms. Also the excess fluorine atoms were perceived to fill the dangling bonds at the grain boundaries, providing certain passivation effect from oxygen to be chemisorbed. In conclusion, FZO films with good electrical conductivity due to large Hall mobility could be obtained by sputtering of ZnO target in CF_4 gas mixture and subsequent annealing in vacuum. Considering the beneficial effect of fluorine doping into ZnO such as low light scattering, i.e. low absorption loss and high Hall mobility, further search for a proper method of increasing doping efficiency in FZO films formed by sputtering would provide a possibility of obtaining excellent TCO films for solar applications.

Acknowledgments

This study was partially supported by a grant from the Fundamental R&D Program for Core Technology of Materials funded by the Ministry of Commerce, Industry and Energy, Republic of Korea.

References

[1] J.F. Carlin Jr., US Geological Survey, Mineral Commodity Summaries, Jan. 2006.
[2] T. Minami, New n-type transparent conducting oxides, MRS Bull. 25 (2000) 38–44.
[3] K. Ellmer, Resistivity of polycrystalline zinc oxide films: current status and physical limit, J. Phys. D: Appl. Phys. 34 (2001) 3097–3108.
[4] S. Faÿ, U. Kroll, C. Bucher, E. Vallat-Sauvain, A. Shah, Low pressure chemical vapour deposition of ZnO layers for thin-film solar cells: temperature-induced morphological changes, Sol. Energy Mater. Sol. Cells 86 (2005) 385–397.
[5] J. Krč, M. Zeman, O. Kluth, F. Smole, M. Topič, Effect of surface roughness of ZnO:Al films on light scattering in hydrogenated amorphous silicon solar cells, Thin Solid Films 426 (2003) 296–304.
[6] R. Groenen, J.L. Linden, H.R.M. van Lierop, D.C. Schram, A.D. Kuypers, M.C.M. van de Sanden, An expanding thermal plasma for deposition of surface textured ZnO:Al with focus on thin film solar cell applications, Appl. Surf. Sci. 173 (2001) 40–43.
[7] S.-M. Park, T. Ikegami, K. Ebihara, Effects of substrate temperature on the properties of Ga-doped ZnO by pulsed laser deposition, Thin Solid Films 513 (2006) 90–94.
[8] S. Kishimoto, T. Yamada, K. Ikeda, H. Makino, T. Yamamoto, Effects of oxygen partial pressure on film growth and electrical properties of undoped ZnO films with thickness below 100 nm, Surf. Coat. Technol. 201 (2006) 4000–4003.
[9] J. Hu, R.G. Gordon, Textured fluorine-doped ZnO thin films by atmospheric pressure chemical vapor deposition and their use in amorphous silicon solar cells, Sol. Cells 30 (1991) 437–450.
[10] R.G. Gordon, Criteria for choosing transparent conductor, MRS Bull. 25 (2000) 52–57.
[11] R.G. Gordon, R. Broomhall-Dillard, X. Liu, D. Pang, J. Barton, Transparent conductors and barrier layers for thin film solar cells, National Renewable Energy laboratory Technical Report, NREL/SR-520-31379, 15 June 2001.
[12] M.L. de la Olivera, A. Maldonado, R. Asomoza, O. Solorza, D.R. Acosta, Characteristics of ZnO:F thin films obtained by chemical spray. Effect of the molarity and the doping concentration, Thin Solid Films 394 (2001) 241–248.
[13] M.L. de la Olivera, A. Maldonado, R. Asomoza, M. Melendez-Lira, Effect of the substrate temperature and acidity of the spray solution on the physical

properties of F-doped ZnO thin films deposited by chemical spray, Sol. Energy Mater. Sol. Cell 71 (2002) 61–71.
[14] T. Miyata, S. Ida, T. Minami, High-rate deposition of ZnO thin films by vacuum arc plasma evaporation, J. Vac. Sci. Technol. A 21 (4) (2003) 1404–1408.
[15] T. Minami, S. Ida, T. Miyata, Y. Minamoto, Transparent conducting ZnO thin films deposited by vacuum arc plasma evaporation, Thin Solid Films 445 (2003) 268–273.
[16] H.Y. Xu, Y.C. Liu, R. Mu, C.L. Shao, Y.M. Lu, D.Z. Shen, X.W. Fan, F-doping effects on electrical and optical properties of ZnO nanocrystalline films, Appl. Phys. Lett. 86 (2005) 123107-1–123107-3.
[17] Y. Shigesato, N. Shin, M. Kamei, P.K. Song, I. Yasui, Study on fluorine-doped indium oxide films deposited by rf magnetron sputtering, Jpn. J. Appl. Phys. 29 (2000) 6422–6426.
[18] R.C. Weast (Ed.), Handbook of Chemistry and Physics, 61st ed., CRC Press, Boca Raton, FL, 1980-1981, p. F223.
[19] D.L. Flamm, in: D.M. Manos, D.L. Flamm (Eds.), Plasma Etching, Academic press, San Diego, CA, 1988, p. 133.
[20] B. Stjerna, E. Olsson, C.G. Granqvist, Optical and electrical properties of radio frequency sputtered tin oxide films doped with oxygen vacancies, F, Sb, or Mo, J. Appl. Phys. 76 (1994) 3797.
[21] V. Srikant, D.R. Clarke, On the optical band gap of zinc oxide, J. Appl. Phys. 83 (1998) 5447.
[22] B.E. Sernelius, K.-F. Berggren, Z.-C. Jin, I. Hamberg, C.G. Granqvist, Band-gap tailoring of ZnO by means of heavy Al doping, Phys. Rev. B 37 (1988) 10244–10248.
[23] JCPDS number 36-1451, International Center for Diffraction Data v.130 (1997).
[24] A. Sanchez-Juareza, A. Tiburcio-Silverb, A. Ortizc, E.P. Zironid, J. Rickards, Electrical and optical properties of fluorine-doped ZnO thin films prepared by spray pyrolysis, Thin Solid Films 333 (1998) 196–202.
[25] K.I. Hagemark, L.C. Chacka, Electrical transport properties of Zn doped ZnO, J. Solid. State Chem. 15 (1975) 261.
[26] F. Oba, S.R. Nishitani, H. Adacha, I. Tanaka, Energetics of native defects in ZnO, J. Appl. Phys. 90 (2001) 824.